Fuel 156 (2015) 234–242

Contents lists available at ScienceDirect

Fuel

journal homepage: www.elsevier.com/locate/fuel

Numerical simulation of biomass fast pyrolysis in an auger reactor

Soroush Aramideh [1], Qingang Xiong [1], Song-Charng Kong *, Robert C. Brown

Department of Mechanical Engineering, Iowa State University, Ames, IA 50011, USA

HIGHLIGHTS

- Integrated CFD and chemical kinetic simulations on biomass fast pyrolysis were conducted.
- Both fluidized-bed and auger reactors were studied.
- Simulation results agree well with experimental data and effects of operating conditions were characterized.

GRAPHICAL ABSTRACT

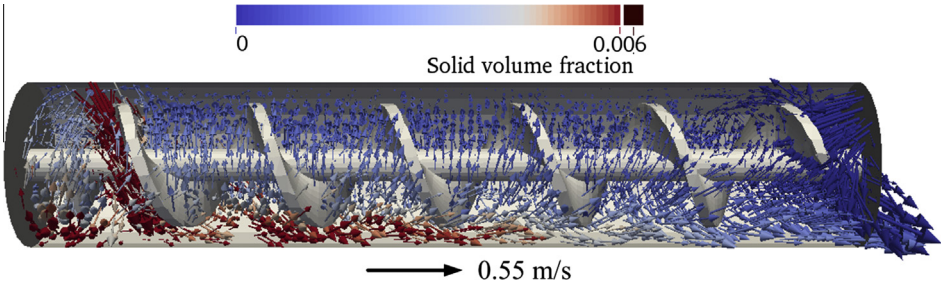

ARTICLE INFO

Article history:
Received 11 February 2015
Received in revised form 13 April 2015
Accepted 16 April 2015
Available online 24 April 2015

Keywords:
Biomass fast pyrolysis
Multi-fluid model
Rotating reference frame
Fluidized bed
Auger reactor

ABSTRACT

Fast pyrolysis is an effective means of converting solid low-energy density biomass to intermediate energy products, such as bio-oil. In this study, computational fluid dynamics (CFD) simulations of the biomass fast pyrolysis processes in both the fluidized-bed and the auger reactors were conducted. The numerical results were validated by experimental data. Materials of all phases were modeled as interpenetrating continua by use of a multi-fluid model. Chemical reactions were simulated using a multi-step reaction mechanism that considers multiple compounds in biomass and various gaseous species in the reactor. In the study of biomass fast pyrolysis in the fluidized-bed reactor, CFD simulation results were analyzed to obtain the average residence time of materials in the reactor. This residence time was used as the time for chemical reactions in estimating the final product yields. The estimated product yields agreed well with the experimental data. To simulate the complex geometry and fluid dynamics in the auger reactor, a numerical approach based on a rotating reference frame was incorporated into the multi-fluid model to account for the auger rotation. Good levels of agreement between the predicted and measured product yields were obtained. A parametric study was conducted to characterize the effects of operating conditions on product yields. The study shows that the optimal wall temperature for maximum tar production was approximately 823 K. The tar yield decreased with increased pre-treatment temperature of the biomass feedstock. It was also found that increased inlet nitrogen flow rate was beneficial to tar yield, while increased biomass feed rate had a negative effect on tar production.

1. Introduction

Developing alternative and clean energy sources has become increasingly urgent because of environmental concerns. Biomass, because of its abundant supply and low life-cycle carbon emissions, is an important renewable energy source. Fast pyrolysis, a thermochemical process that decomposes low-energy density organic materials in the absence of oxygen, is a promising approach to converting raw biomass into high-energy density bio-oil and combustible gases [1]. Because of this attractive feature, biomass fast pyrolysis has received great attention from both industry and the scientific community [2]. However, because of the complex nature of biomass fast pyrolysis in chemical reactors, current technologies for converting biomass to bio-oil via fast

* Corresponding author. Tel.: +1 515 294 3244.
E-mail address: kong@iastate.edu (S.-C. Kong).
[1] Equal contributors.

http://dx.doi.org/10.1016/j.fuel.2015.04.038
0016-2361/

pyrolysis still face many challenges. The multiphase flow in the biomass fast pyrolyzer is highly complex, and it is rather difficult to optimize the reactor operating conditions for desirable product yields [3]. In addition, because of the multiscale nature of the biomass feedstock, the performance of a reactor depends significantly on the geometrical characteristics of the biomass particles [4].

Computational fluid dynamics (CFD) simulations, in which conservation laws and equations are employed to describe the complicated multiphase fluid dynamics and chemical reactions, has helped develop understanding of the complex multiphase flows and biomass fast pyrolysis process [5–22]. Compared with experimental approaches [23–25], CFD can effectively provide detailed information on the processes occurring in the reactor. Considerable costs and time can be saved by use of CFD for reactor design, optimization, and scaling up. Moreover, CFD has the advantage of being useful in exploring detailed processes occurring in harsh reactor environments that have posed great challenges to researchers.

For biomass fast pyrolysis simulation, CFD has been applied mainly to the fluidized-bed reactor because of the simple geometry and widespread applications of this reactor [26–36]. Fluidized beds can provide excellent gas–solid mixing and heat transfer. Because of the simple geometry, temperature control and operation of fluidized beds are more straightforward than for other types of reactors. Therefore, in the research discussed in this paper, we continued our previous studies [37–39] on CFD simulation of biomass fast pyrolysis in a bubbling fluidized-bed reactor and conducted further analyses of the simulation results to characterize the pyrolysis product yields.

The auger reactor, a novel type of reactor, has attracted much interest for biomass fast pyrolysis application [40,41]. Auger reactors can be operated continuously with little or no carrier gas. Along with the rotation of one or multiple screw conveyors in the reactor, materials of different phases are mixed to enhance heat transfer among solids, gases, and the reactor wall. The resulting biochar particles are mechanically transported toward the reactor exit by the rotating screw to empty the reactor such that subsequent biomass particles can be fed and pyrolyzed. Because of the rather complex geometry and motion of the screw, the numerical analysis of biomass fast pyrolysis in auger reactors is very rare in the literature. It appears that there has been no report on multi-dimensional CFD simulation of biomass fast pyrolysis in auger reactors using comprehensive numerical models. Nonetheless, CFD simulation is highly important for the design and optimization of auger reactors to achieve effective biomass fast pyrolysis, since it is very costly to conduct comprehensive experiments. Therefore, in this paper, numerical models are introduced for simulating a laboratory-scale auger reactor using CFD.

In this work, a multi-fluid model (MFM) was employed to simulate the multiphase fluid dynamics and a multi-component multi-step reaction kinetics mechanism was applied to describe the biomass fast pyrolysis reactions. The rotation of the screw in the auger reactor was simulated based on the concept of a rotating reference frame. The numerical results were compared with experimental data, and the effects of operating conditions were quantified.

2. Numerical models

2.1. Multi-fluid model

On the basis of our previous studies [37–39], a multi-fluid model was used to simulate the hydrodynamics and heat transfer in the fast pyrolysis reactor. In a MFM, all phases are treated as interpenetrating continua, and the governing equations for mass, momentum, and energy conservations are solved to obtain the spatiotemporal evolutions of the phase volume fraction, velocity, temperature, and species mass fraction. The conservation equations are summarized in Table 1. Various numerical models for gas–solid drag force and heat transfer are summarized in Table 2. A detailed description of the model used in this study can be found in previous publications [37,39].

2.2. Rotating reference frame

The motion of the rotating screw in the auger reactor was modeled using the so-called rotating reference frame (RRF) [42]. In a RRF, the velocity and acceleration of a rotating object in an inertial coordinate can be expressed by the corresponding velocity and acceleration obtained from a rotating coordinate. The idea of RRF can be described as follows. For a rotating axis with a constant angular velocity $\boldsymbol{\omega}$, the velocity and acceleration of a point at a distance $\boldsymbol{r}$ from the rotating axis can be expressed in the following.

$$\boldsymbol{U}_{inertial}(\boldsymbol{r},t) = \boldsymbol{U}_{rotating}(\boldsymbol{r},t) + \boldsymbol{\omega}\times\boldsymbol{r}, \tag{1}$$

$$\frac{d\boldsymbol{U}_{inertial}(\boldsymbol{r},t)}{dt} = \frac{d\boldsymbol{U}_{rotating}(\boldsymbol{r},t)}{dt} + 2\boldsymbol{\omega}\times\boldsymbol{U}_{rotating}(\boldsymbol{r},t) + \boldsymbol{\omega}\times(\boldsymbol{\omega}\times\boldsymbol{r})$$

Based on Eq. (1), the momentum equation, as listed in Table 1, for the gas phase in the rotating coordinate can be written as

Table 1
Governing equations of the MFM in this study.

Gas phase	Solid phase
Continuity equation $\frac{\partial \alpha_g \rho_g}{\partial t} + \nabla\cdot(\alpha_g\rho_g\boldsymbol{U}_g) = R_g$	Continuity equation $\frac{\partial \alpha_{sm} \rho_{sm}}{\partial t} + \nabla\cdot(\alpha_{sm}\rho_{sm}\boldsymbol{U}_{sm}) = R_{sm}$
Momentum equation $\frac{\partial(\alpha_g\rho_g\boldsymbol{U}_g)}{\partial t} + \nabla\cdot(\alpha_g\rho_g\boldsymbol{U}_g\boldsymbol{U}_g) = \nabla\cdot\boldsymbol{\tau}_g - \alpha_g\nabla p + \sum_{m=1}^{M}\beta_{gsm}(\boldsymbol{U}_{sm}-\boldsymbol{U}_g) + \sum_{m=1}^{M}\psi_{gsm} + \alpha_g\rho_g\boldsymbol{g}$	Momentum equation $\frac{\partial(\alpha_{sm}\rho_{sm}\boldsymbol{U}_{sm})}{\partial t} + \nabla\cdot(\alpha_{sm}\rho_{sm}\boldsymbol{U}_{sm}\boldsymbol{U}_{sm}) = \nabla\cdot\boldsymbol{\tau}_{sm} - \alpha_{sm}\nabla p + \beta_{gsm}(\boldsymbol{U}_g-\boldsymbol{U}_{sm}) + \sum_{l=1,l\neq m}^{M}\beta_{slm}(\boldsymbol{U}_{sl}-\boldsymbol{U}_{sm}) + \psi_{gsm} + \alpha_{sm}\rho_{sm}\boldsymbol{g}$
Stress–strain tensor: $\boldsymbol{\tau}_g = 2\alpha_g\mu_g\boldsymbol{D}_g + \alpha_g\lambda_g tr(\boldsymbol{D}_g)\boldsymbol{I}$	Stress–strain tensor: $\boldsymbol{\tau}_{sm} = -p_{sm}\boldsymbol{I} + 2\alpha_{sm}\mu_{sm}\boldsymbol{D}_{sm} + \alpha_{sm}\lambda_{sm}tr(\boldsymbol{D}_{sm})\boldsymbol{I}$
	Solid phase properties obtained using KTGF [51]
Energy equation $\frac{\partial(\alpha_g\rho_g C_{pg}T_g)}{\partial t} + \nabla\cdot(\alpha_g\rho_g C_{pg}T_g\boldsymbol{U}_g) = \nabla\cdot\boldsymbol{q}_g + \sum_{m=1}^{M}h_{gsm}(T_{sm}-T_g) + H_g$	Energy equation $\frac{\partial(\alpha_{sm}\rho_{sm}C_{sm}T_{sm})}{\partial t} + \nabla\cdot(\alpha_{sm}\rho_{sm}C_{psm}T_{sm}\boldsymbol{U}_{sm}) = \nabla\cdot\boldsymbol{q}_{sm} + h_{gsm}(T_g-T_{sm}) + H_{sm}$
Conductive heat flux: $\boldsymbol{q}_g = \alpha_g\kappa_g\nabla T_g$	Conductive heat flux: $\boldsymbol{q}_{sm} = \alpha_{sm}\kappa_{sm}\nabla T_{sm}$
Species equation $\frac{\partial \alpha_g\rho_g Y_{gk}}{\partial t} + \nabla\cdot(\alpha_g\rho_g Y_{gk}\boldsymbol{U}_g) = j_{gk} + R_{gk}$	Species equation $\frac{\partial \alpha_{sm}\rho_{sm} Y_{smk}}{\partial t} + \nabla\cdot(\alpha_{sm}\rho_{sm} Y_{smk}\boldsymbol{U}_{sm}) = R_{smk}$
Diffusive flux: $j_{gk} = \alpha_g\rho_g\boldsymbol{D}_{gk}\nabla Y_{jk}$	